Halo-independent tests relevant for inelastic dark matter scattering

Nassim Bozorgnia

MAX-PLANCK-INSTITUT FÜR KERNPHYSIK

Based on work done with J. Herrero-Garcia, T. Schwetz, and J. Zupan

invisibles
neutrinos, dark matter & dark energy physics

Direct dark matter detection

- Assuming ***elastic*** spin-independent scattering, strong tension between DAMA signal and XENON100 bound:

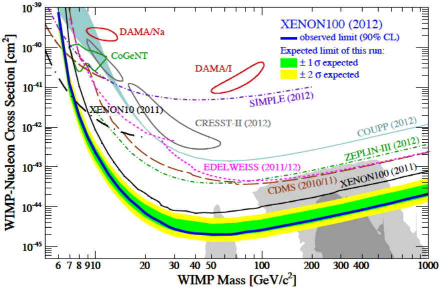

XENON100 Collaboration, 1207.5988

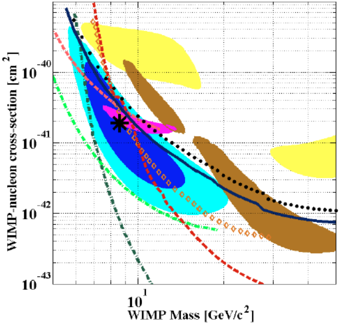

CDMS Collaboration, 1304.4279

Direct dark matter detection

- Assuming ***elastic*** spin-independent scattering, strong tension between DAMA signal and XENON100 bound:

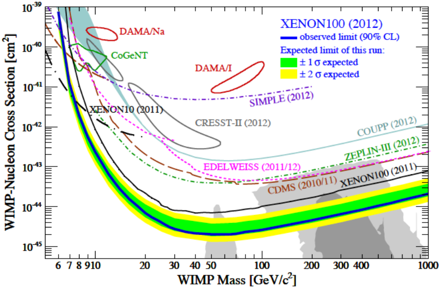

XENON100 Collaboration, 1207.5988

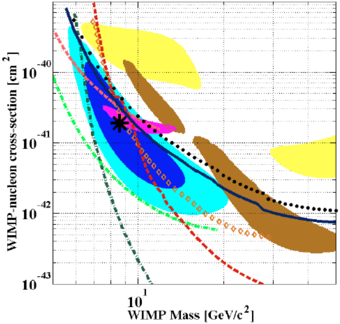

CDMS Collaboration, 1304.4279

- These kind of plots assume the "Standard Halo Model": isothermal sphere with an isotropic Maxwell-Boltzmann velocity distribution.

Direct dark matter detection

- **Inelastic** scattering: DM particle χ scatters to an excited state χ^* with mass difference $\delta = m_\chi^* - m_\chi \sim \mathcal{O}(100)$ keV
- In **DAMA NaI**: scattering off heavy iodine is favored.

Direct dark matter detection

- **Inelastic** scattering: DM particle χ scatters to an excited state χ^* with mass difference $\delta = m_\chi^* - m_\chi \sim \mathcal{O}(100)$ keV
- In **DAMA NaI**: scattering off heavy iodine is favored.
- Are different experiments consistent? The answer depends significantly on the halo model assumptions.
- In the SHM and under specific assumptions for the DM halo, also the inelastic scattering explanation of the DAMA signal is in tension with the XENON100 bound.

Direct dark matter detection

- **Inelastic** scattering: DM particle χ scatters to an excited state χ^* with mass difference $\delta = m_\chi^* - m_\chi \sim \mathcal{O}(100)$ keV
- In **DAMA NaI**: scattering off heavy iodine is favored.
- Are different experiments consistent? The answer depends significantly on the halo model assumptions.
- In the SHM and under specific assumptions for the DM halo, also the inelastic scattering explanation of the DAMA signal is in tension with the XENON100 bound.
- We will check this conclusion in a halo-independent way **(arXiv:1305.3575)**.

Direct dark matter detection

- WIMP-nucleus collision:

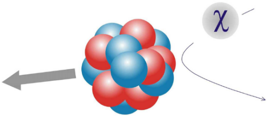

- Minimum WIMP speed required to produce a recoil energy E_R:

$$v_m = \sqrt{\frac{1}{2m_A E_R}}\left(\frac{m_A E_R}{\mu_{\chi A}} + \delta\right)$$

Direct dark matter detection

- WIMP-nucleus collision:

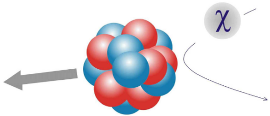

- Minimum WIMP speed required to produce a recoil energy E_R:

$$v_m = \sqrt{\frac{1}{2m_A E_R}}\left(\frac{m_A E_R}{\mu_{\chi A}} + \delta\right)$$

- For inelastic scattering, $v_m \sim v_{\rm esc}$ $\Rightarrow$ experiment probes the tails of the DM velocity distribution, where halo substructures are expected $\Rightarrow$ important to develop halo-independent methods

The differential event rate

- The differential event rate (event/keV/kg/day):

$$R(E_R, t) = \frac{\rho_\chi}{m_\chi} \frac{1}{m_A} \int_{v > v_m} d^3 v \frac{d\sigma_A}{dE_R} \; v \; f_{\rm det}(\mathbf{v}, t)$$

The differential event rate

- The differential event rate (event/keV/kg/day):

$$R(E_R, t) = \frac{\rho_\chi}{m_\chi} \frac{1}{m_A} \int_{v > v_m} d^3 v \frac{d\sigma_A}{dE_R} \; v \; f_{\rm det}(\mathbf{v}, t)$$

- For the standard spin-independent and spin-dependent scattering:

$$R(E_R, t) = \frac{\rho_\chi \sigma_0 F^2(E_R)}{2 m_\chi \mu_{\chi A}^2} \; \eta(v_m, t)$$

where

$$\eta(v_m, t) \equiv \int_{v > v_m} d^3 v \; \frac{f_{\rm det}(\mathbf{v}, t)}{v}$$

The differential event rate

- The differential event rate (event/keV/kg/day):

$$R(E_R, t) = \frac{\rho_\chi}{m_\chi} \frac{1}{m_A} \int_{v>v_m} d^3v \frac{d\sigma_A}{dE_R} \; v \; f_{\rm det}(\mathbf{v}, t)$$

- For the standard spin-independent and spin-dependent scattering:

$$R(E_R, t) = \frac{\rho_\chi \sigma_0 F^2(E_R)}{2 m_\chi \mu_{\chi A}^2} \; \eta(v_m, t)$$

where

$$\eta(v_m, t) \equiv \int_{v>v_m} d^3v \; \frac{f_{\rm det}(\mathbf{v}, t)}{v}$$

$$f_{\rm det}(\mathbf{v}, t) = f_{\rm sun}(\mathbf{v} + \mathbf{v}_e(t)) \quad , \quad v_e \approx 30 \text{ km/s}$$

Bound on the annual modulation amplitude

- **Basic assumption:** $f_{\rm sun}(\mathbf{v})$ is constant on timescales of 1 yr, and on the scale of the Sun-Earth distance $\Rightarrow$ only time dependence due to $\mathbf{v}_e(t)$

$$\eta(v_m, t) = \int_{v>v_m} d^3v \, \frac{f_{\rm sun}(\mathbf{v} + \mathbf{v}_e(t))}{v}$$

Bound on the annual modulation amplitude

- **Basic assumption:** $f_{\rm sun}(\mathbf{v})$ is constant on timescales of 1 yr, and on the scale of the Sun-Earth distance $\Rightarrow$ only time dependence due to $\mathbf{v}_e(t)$

$$\eta(v_m, t) = \int_{v>v_m} d^3v \, \frac{f_{\rm sun}(\mathbf{v} + \mathbf{v}_e(t))}{v}$$

- Using the fact that v_e is small, one can expand the halo integral in powers of v_e

$$\eta(v_m, t) = \underbrace{\eta_0(v_m)}_{\text{unmodulated}} + \underbrace{A_\eta(v_m)}_{\text{annual mod. ampl.}} \cos 2\pi[t - t_0(v_m)] + \mathcal{O}(v_e^2)$$

Bound on the annual modulation amplitude

- **Basic assumption:** $f_{\rm sun}(\mathbf{v})$ is constant on timescales of 1 yr, and on the scale of the Sun-Earth distance $\Rightarrow$ only time dependence due to $\mathbf{v}_e(t)$

$$\eta(v_m, t) = \int_{v>v_m} d^3v \, \frac{f_{\rm sun}(\mathbf{v} + \mathbf{v}_e(t))}{v}$$

- Using the fact that v_e is small, one can expand the halo integral in powers of v_e

$$\eta(v_m, t) = \underbrace{\eta_0(v_m)}_{\text{unmodulated}} + \underbrace{A_\eta(v_m)}_{\text{annual mod. ampl.}} \cos 2\pi[t - t_0(v_m)] + \mathcal{O}(v_e^2)$$

- The modulation amplitude can be bounded in terms of the unmodulated halo integral

$$\boxed{\int_{u_{\rm min}}^{u_{\rm max}} dv A_\eta(v)(v - u_{\rm min}) < \frac{v_e}{2}\left(3 - \frac{u_{\rm min}^2}{u_{\rm max}^2}\right) \int_{u_{\rm min}}^{u_{\rm max}} dv \, \eta_0(v)}$$

$[u_{\rm min}, u_{\rm max}]$: range in minimal velocities probed by the experiment

Bound on the annual modulation amplitude

$$\boxed{\int_{u_{\rm min}}^{u_{\rm max}} dv\, A_\eta(v)(v - u_{\rm min}) < \frac{v_e}{2}\left(3 - \frac{u_{\rm min}^2}{u_{\rm max}^2}\right) \int_{u_{\rm min}}^{u_{\rm max}} dv\, \eta_0(v)}$$

- The bound depends on m_χ, $q(E_R)$, and $F^2(E_R)$, but not on ρ_χ, σ_p, and $v_{\rm esc}$.
- The l.h.s. and r.h.s. can refer to different experiments.

Bound on the annual modulation amplitude

$$\boxed{\int_{u_{\min}}^{u_{\max}} dv\, A_\eta(v)(v-u_{\min}) < \frac{v_e}{2}\left(3-\frac{u_{\min}^2}{u_{\max}^2}\right)\int_{u_{\min}}^{u_{\max}} dv\, \eta_0(v)}$$

- The bound depends on m_χ, $q(E_R)$, and $F^2(E_R)$, but not on ρ_χ, σ_p, and $v_{\rm esc}$.
- The l.h.s. and r.h.s. can refer to different experiments.

Applying the bound to data:

- Calculate the **l.h.s.** using modulation data from **DAMA**.
- Calculate the **r.h.s.** using an upper bound on η_0 from the observed number of events in **XENON100**.

Bound on the annual modulation amplitude

- For inelastic scattering, $\Delta v = u_{\rm max} - u_{\rm min}$ is small.

Bound on the annual modulation amplitude

- For inelastic scattering, $\Delta v = u_{\rm max} - u_{\rm min}$ is small.

- expansion parameter is $v_e/\Delta v$ $\Rightarrow$ can become of order one.

Bound on the annual modulation amplitude

- For inelastic scattering, $\Delta v = u_{\max} - u_{\min}$ is small.

- expansion parameter is $v_e/\Delta v$ $\Rightarrow$ can become of order one.

- The expansion breaks down for $v_e/\Delta v \gtrsim 1$

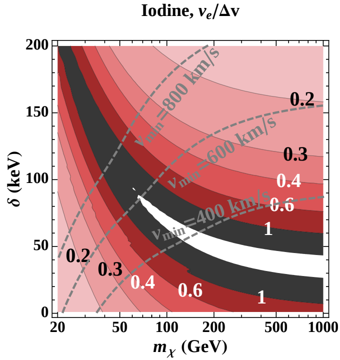

Bound on the annual modulation amplitude

- For inelastic scattering, $\Delta v = u_{\rm max} - u_{\rm min}$ is small.

- expansion parameter is $v_e/\Delta v$ $\Rightarrow$ can become of order one.

- The expansion breaks down for $v_e/\Delta v \gtrsim 1$

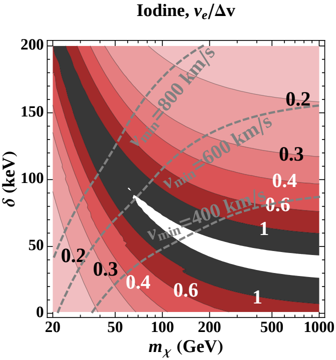

- In regions where our expansion breaks down, we can use a "trivial bound": the amplitude of the annual modulation has to be smaller than the unmodulated rate: $A_\eta \leq \eta_0$ (valid in the full parameter space).

Bound on the annual modulation amplitude

- "trivial bound": $(A_\eta \leq \eta_0)$

$$\frac{v_e}{2}\left(3 - \frac{u_{\min}^2}{u_{\max}^2}\right)\int_{u_{\min}}^{u_{\max}} dv\, A_\eta(v) < \frac{v_e}{2}\left(3 - \frac{u_{\min}^2}{u_{\max}^2}\right)\int_{u_{\min}}^{u_{\max}} dv\, \eta_0(v)$$

- general bound:

$$\int_{u_{\min}}^{u_{\max}} dv\, A_\eta(v)(v - u_{\min}) < \frac{v_e}{2}\left(3 - \frac{u_{\min}^2}{u_{\max}^2}\right)\int_{u_{\min}}^{u_{\max}} dv\, \eta_0(v)$$

Shape test

- Work in v_m space to directly compare different experiments
  $\Rightarrow$ translate physical observables in E_R to v_m.

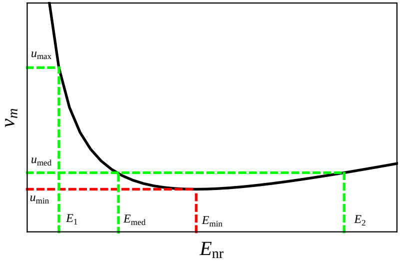

$$v_m = \sqrt{\frac{1}{2m_A E_R}} \left(\frac{m_A E_R}{\mu_{\chi A}} + \delta \right)$$

- Non-unique relation between v_m and E_R
  $\Rightarrow$ complications for inelastic scattering

Shape test

- Work in v_m space to directly compare different experiments
  $\Rightarrow$ translate physical observables in E_R to v_m.

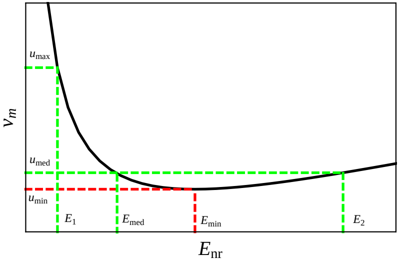

$$v_m = \sqrt{\frac{1}{2m_A E_R}}\left(\frac{m_A E_R}{\mu_{\chi A}} + \delta\right)$$

- Non-unique relation between v_m and E_R
  $\Rightarrow$ complications for inelastic scattering

- Numerically compute integrals such as: $\int_{u_{\rm min}}^{u_{\rm max}} dv A_\eta(v)(v - u_{\rm min})$

Shape test

- Work in v_m space to directly compare different experiments
  $\Rightarrow$ translate physical observables in E_R to v_m.

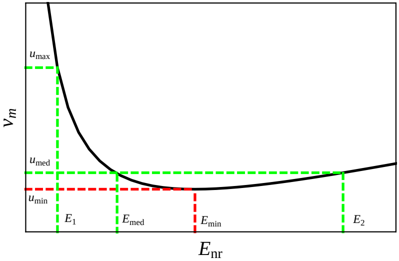

$$v_m = \sqrt{\frac{1}{2 m_A E_R}} \left(\frac{m_A E_R}{\mu_{\chi A}} + \delta \right)$$

- Non-unique relation between v_m and E_R
  $\Rightarrow$ complications for inelastic scattering

- Numerically compute integrals such as: $\int_{u_{\min}}^{u_{\max}} dv A_\eta(v)(v - u_{\min})$

- The interval $[u_{\min}, u_{\mathrm{med}}]$ corresponds to two energy regions: $[E_{\mathrm{med}}, E_{\min}]$ and $[E_{\min}, E_2]$.

Shape test

- Work in v_m space to directly compare different experiments
  $\Rightarrow$ translate physical observables in E_R to v_m.

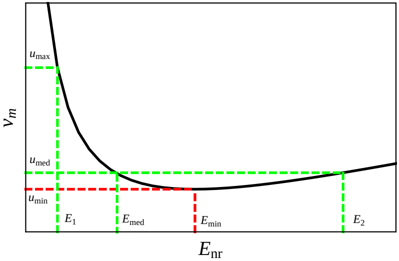

$$v_m = \sqrt{\frac{1}{2m_A E_R}}\left(\frac{m_A E_R}{\mu_{\chi A}} + \delta\right)$$

- Non-unique relation between v_m and E_R
  $\Rightarrow$ complications for inelastic scattering

- Numerically compute integrals such as: $\int_{u_{\min}}^{u_{\max}} dv A_\eta(v)(v - u_{\min})$

- The interval $[u_{\min}, u_{\rm med}]$ corresponds to two energy regions: $[E_{\rm med}, E_{\min}]$ and $[E_{\min}, E_2]$.

- if DM scatters inelastically, $I_a = \int_{E_{\rm med}}^{E_{\min}}$ and $I_b = \int_{E_{\min}}^{E_2}$ should give the same value.

Shape test

- Test the hypothesis that the signal is due to inelastic DM scattering by requiring that I_a and I_b agree within experimental errors.

Shape test

- Test the hypothesis that the signal is due to inelastic DM scattering by requiring that I_a and I_b agree within experimental errors.

- compute the difference weighted by the error as obtained from DAMA data:

$$\frac{|I_a - I_b|}{\sqrt{\sigma_a^2 + \sigma_b^2}}$$

Shape test

- Test the hypothesis that the signal is due to inelastic DM scattering by requiring that I_a and I_b agree within experimental errors.
- compute the difference weighted by the error as obtained from DAMA data:

$$\frac{|I_a - I_b|}{\sqrt{\sigma_a^2 + \sigma_b^2}}$$

- a strip in parameter space is excluded at $> 3\sigma$, just requiring a spectral shape of the signal consistent with inelastic scattering.

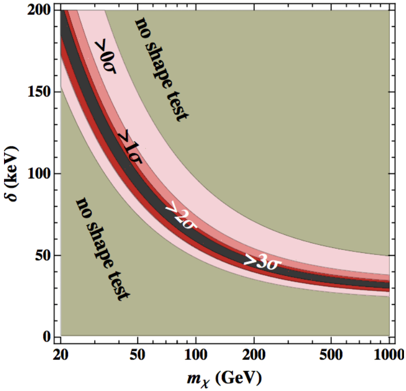

Numerical results

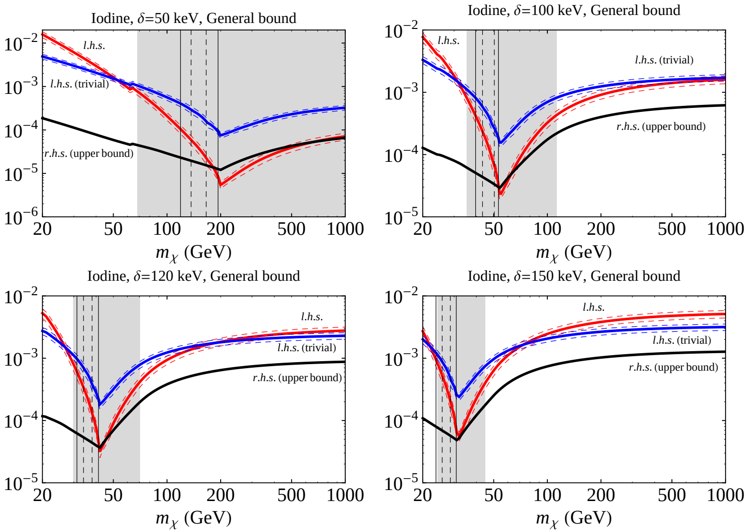

Numerical results

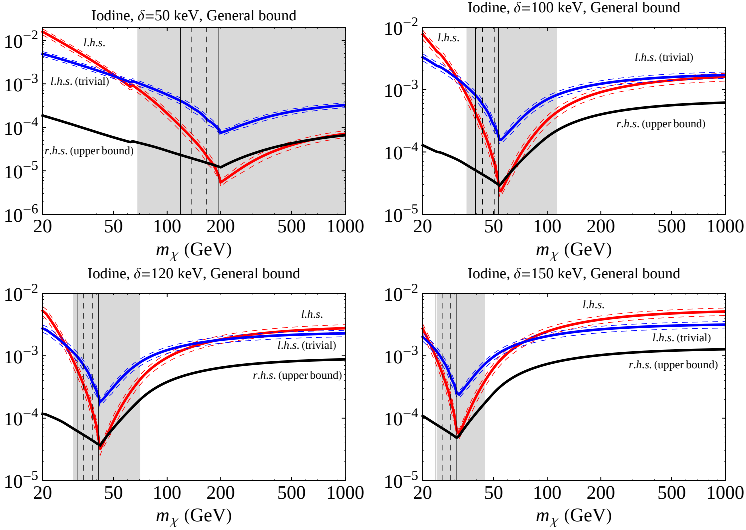

- The bound is strongly violated, disfavoring an inelastic scattering interpretation of the DAMA signal halo independently.

Summary

- We generalized the method to compare different experiments **independent of assumptions on the DM distribution** to the case of inelastic scattering.

Summary

- We generalized the method to compare different experiments **independent of assumptions on the DM distribution** to the case of inelastic scattering.
- Three different tests for the consistency of the inelastic interpretation of the DAMA signal and its tension with XENON100:
  - the bound on the annual modulation amplitude based on an expansion of the halo integral in v_e.
  - the trivial bound obtained by the requirement that $A_\eta \leq \eta_0$.
  - the shape test based on the predicted shape of the signal.

Summary

- We generalized the method to compare different experiments **independent of assumptions on the DM distribution** to the case of inelastic scattering.
- Three different tests for the consistency of the inelastic interpretation of the DAMA signal and its tension with XENON100:
  - the bound on the annual modulation amplitude based on an expansion of the halo integral in v_e.
  - the trivial bound obtained by the requirement that $A_\eta \leq \eta_0$.
  - the shape test based on the predicted shape of the signal.
- We confirmed in a halo-independent way that the inelastic scattering explanation of the DAMA signal is strongly disfavored by XENON100.

Summary

- We generalized the method to compare different experiments **independent of assumptions on the DM distribution** to the case of inelastic scattering.
- Three different tests for the consistency of the inelastic interpretation of the DAMA signal and its tension with XENON100:
  - the bound on the annual modulation amplitude based on an expansion of the halo integral in v_e.
  - the trivial bound obtained by the requirement that $A_\eta \leq \eta_0$.
  - the shape test based on the predicted shape of the signal.
- We confirmed in a halo-independent way that the inelastic scattering explanation of the DAMA signal is strongly disfavored by XENON100.
- The methods developed will provide a valuable consistency check for an inelastic scattering interpretation of any future DM signal.

Additional slides

Upper bound on η_0

- The expected number of events in a recoil energy interval $[E_1, E_2]$

$$N^{\rm pred}_{[E_1,E2]} = C \int_0^\infty dE_R F^2(E_R) G_{[E_1,E_2]} \eta_0(v_m(E_R))$$

- Since η_0 is a decreasing function, at a given v_m, the minimum number of events is obtained for $\eta_0(v) = \eta_0(v_m)\Theta(v_m - v)$,

$$N^{\rm pred}_{[E_1,E2]} \geq C \eta_0(v_m) \int_{E_-}^{E_+} dE_R F^2(E_R) G_{[E_1,E_2]}$$

- We can obtain an upper bound on $\eta_0(v_m)$ from the observed number of events in XENON100